

Cite this: *CrystEngComm*, 2012, 14, 8010–8016

www.rsc.org/crystengcomm

PAPER

## Achieving molecular stability of racemic 4-*O*-benzyl-*myo*-inositol-1,3,5-orthoformate through crystal formation†

Richa Sardesai,<sup>a</sup> Shobhana Krishnaswamy<sup>b</sup> and Mysore S. Shashidhar<sup>\*a</sup>

Received 27th April 2012, Accepted 28th August 2012

DOI: 10.1039/c2ce26199e

Molecular stability of racemic 4-*O*-benzyl-*myo*-inositol-1,3,5-orthoformate, an early intermediate during the synthesis of phosphoinositols, depends on the phase in which it is stored. This orthoformate is stable when stored in the crystalline form or as solution in common organic solvents. The former has eluded chemists since the preparation of this benzyl ether two decades ago. The difficulty in obtaining crystals of this orthoformate is due to the cleavage of the orthoformate moiety during storage in the gummy state. Dimorphs (form I and form II) of crystalline racemic 4-*O*-benzyl-*myo*-inositol-1,3,5-orthoformate, were obtained when the gummy sample was stored over extended periods of time. Form I crystals could be obtained consistently, by crystallization of a frozen (−20 °C) solid sample, from a solution of dichloromethane–light petroleum. The two crystal forms display dissimilar patterns of hydrogen bonding and molecular assembly in the solid-state.

### Introduction

4-*O*-substituted-*myo*-inositol-1,3,5-orthoesters are versatile intermediates for the preparation of biologically relevant inositol derivatives.<sup>1–4</sup> In particular, racemic 4-*O*-benzyl-*myo*-inositol-1,3,5-orthoformate (**4**) has been utilized for the synthesis of phosphoinositols and their analogs. Phosphoinositols play a significant role in cellular signal transduction pathways, and impairment of the *myo*-inositol cycle has been implicated in several diseases.<sup>5–8</sup> We had to prepare, store and use relatively larger amounts of **4** as a part of an ongoing program on the chemistry of inositols.<sup>9</sup> We were intrigued to realize that **4** was stable when stored as a solution in common organic solvents, but did not stay pure when stored as a gum at ambient temperature. A survey of the literature revealed that, while the physical state of **4** at ambient conditions was mentioned as a gum in some reports,<sup>10,11</sup> most others did not mention the physical state (or the purity) of the sample used for further synthetic transformations. It was also surprising to note that while many 4-*O*-substituted *myo*-inositol-1,3,5-orthoesters exist as solids or crystalline compounds under ambient conditions,<sup>12,13</sup> the benzyl ether **4** was never reported as a solid. Hence we scrutinized the

samples of **4** stored over varying periods of time (days to years) and observed that some samples of **4** exhibited partial degradation of the molecules while a few other samples had crystallized. Subsequently, we could arrive at experimental conditions to obtain good crystals of **4** which prevented molecular degradation on storage.

The results of this investigation showed that the orthoformate **4** undergoes cleavage to the corresponding formyl ester in the gummy state, while it is inert in crystalline and solution states. We had earlier reported<sup>14</sup> an interesting instance of the epimerization of inositol 1,3-bridged acetals, which occurred only in the molten state, but not in the solid and solution states. Encountering such instances of variation of the stability of molecules in different phases reiterates the importance of the effect of molecular aggregation on observed properties attributed to individual molecules.

### Experimental

#### Analysis of the samples of racemic 4-*O*-benzyl-*myo*-inositol-1,3,5-orthoformate (**4**)

Samples of the racemic benzyl ether **4** obtained as a gum (sample **4A**) by a reported<sup>10</sup> procedure, were stored (in sealed containers out of contact with air) for various periods of time and analyzed by IR and NMR spectroscopy (see ESI†). The majority of these samples either stayed as gums (for a few days up to two weeks at ambient temperature, sample **4B**) or turned into a solid (in about four weeks at ambient temperature, or longer duration in a refrigerator, sample **4C**). Samples of **4** (stored below −10 °C for more than 2–3 weeks) formed a shiny solid (sample **4D**) or yielded rectangular plate-like crystals (form I). In another instance, the gum obtained (after slow evaporation of the

<sup>a</sup>Division of Organic Chemistry, National Chemical Laboratory—Council of Scientific and Industrial Research (CSIR), Pashan Road, Pune, 411 008. E-mail: ms.shashidhar@ncl.res.in; Fax: +91-20-25902624; Tel: +91-20-25902055

<sup>b</sup>Center for Materials Characterization, National Chemical Laboratory—Council of Scientific and Industrial Research (CSIR), Pashan Road, Pune, 411 008. Fax: +91-20-25902642; Tel: +91-20-25902252

† Electronic supplementary information (ESI) available: IR and NMR spectra of different samples of **4**, **5** and **6**; PXRD patterns for solid samples of **4**. CCDC reference numbers 848918–848919. For ESI and crystallographic data in CIF or other electronic format see DOI: 10.1039/c2ce26199e

solvent, dichloromethane) was stored at 0–4 °C for 3 months, which resulted in the formation of block-shaped crystals (form II). Infrared and <sup>1</sup>H NMR spectra of these samples are included in the ESI.†

The sample **4C** (0.09 g) on thin layer chromatographic analysis indicated the presence of two compounds. Column chromatography (silica 60–120 mesh, eluent, 1 : 1 ethyl acetate : hexane) of this sample yielded gummy **4** (0.051 g) and an amorphous solid (0.017 g). The latter was acetylated using acetic anhydride (0.08 mL, 0.915 mmol) in pyridine (1 mL) for 48 h at ambient temperature. The solvents were evaporated under reduced pressure and the residue was dissolved in ethyl acetate and washed with dil. HCl, water and brine; the organic layer was dried over anhydrous sodium sulfate. Removal of the solvent under reduced pressure gave the known<sup>15</sup> penta acetate **8** (0.02 g) as a white flaky solid. M.p. 159–160 °C lit.<sup>15</sup> M.p. 162–164 °C.

### Crystallisation of **4**

A freshly prepared gummy sample of **4** (sample **4A**, 0.5 g) was stored at –20 °C for 12 h to obtain a solid (sample **4E** M.p. 84–86 °C). It was dissolved in dichloromethane (4–5 mL). To this solution, light petroleum (boiling range 60–80 °C) was added drop-wise till turbidity appeared and persisted. Minimum amount of dichloromethane was then added drop-wise until a clear solution was obtained. The mouth of the container was covered with perforated aluminium foil and the solution was allowed to stand at ambient temperature. Fine plates (Form I crystals) appeared after 5–6 h; complete crystallization took 48 h. M.p. 86–88 °C. Our attempts to crystallize freshly prepared gummy samples **4A**, without storing at –20 °C failed.

Although we were able to observe the formation of form II crystals (M.p. 90 °C) in some of the stored samples of **4**, we could not develop a procedure to obtain these crystals consistently, perhaps due to the long duration (several months during which **4** progressively decomposes to result in samples of varied purity) necessary for the formation of these crystals.

### Synthesis of racemic 4-*O*-benzyl-*myo*-inositol-1,3,5-orthoacetate (**5**)

To an ice-cooled solution of *myo*-inositol-1,3,5-orthoacetate (**2**, 0.75 g, 3.72 mmol) in dry DMF (15 mL), sodium hydride (0.16 g, 4.09 mmol, 60% suspension in mineral oil) was added, followed by benzyl bromide (0.48 mL, 4.09 mmol). The reaction mixture was stirred at room temperature for 80 min, and then quenched with ice. The solvent was removed under reduced pressure and the residue was diluted with ethyl acetate. The organic layer was washed with dil. HCl, followed by brine, dried over anhydrous sodium sulphate and concentrated. The gum obtained was flash column chromatographed (230–400 mesh silica gel; eluent, 1 : 3 ethyl acetate : light petroleum) to obtain **5** (0.627 g, 58%) as a pale yellow gum. Crystals of **5** could be obtained by slow evaporation of dichloromethane solution at ambient temperature, M.p. 90–94 °C. However, the crystals were soft and sticky, resulting in poor quality X-ray diffraction data. <sup>1</sup>H NMR (CDCl<sub>3</sub>, 200 MHz): δ 7.44–7.27 (m, 5H), 4.67 (dd, *J*<sub>1</sub> = 11.6 Hz, *J*<sub>2</sub> = 13.4 Hz, 2H), 4.45–4.38 (m, 2H), 4.26–4.20 (m, 3H), 4.03 (m, 1H), 3.66 (d, *J* = 10.2 Hz, 1H, D<sub>2</sub>O exchangeable), 3.04 (d, *J* = 11.9 Hz, 1H, D<sub>2</sub>O exchangeable), 1.43 (s, 3H) ppm.

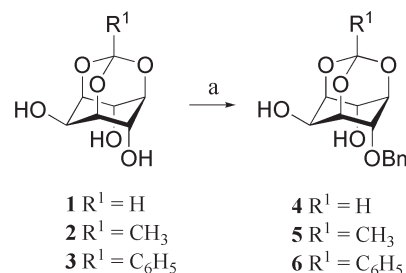
<sup>13</sup>C NMR (CDCl<sub>3</sub>, 50.32 MHz): δ 135.9, 128.9, 128.8, 128.1, 108.7, 75.3, 74.0, 73.0 (CH<sub>2</sub>), 72.8, 67.7, 67.4, 59.8, 24.1.

### Crystallographic details

Single-crystal X-ray intensity measurements for crystals of **4** (form I and form II) were recorded at ambient temperature on a Bruker SMART APEX single crystal X-ray CCD diffractometer with graphite-monochromatized (Mo-Kα = 0.71073 Å) radiation. The X-ray generator was operated at 50 kV and 30 mA. Diffraction data were collected with a ω scan width of 0.3° at different settings of φ (0, 90, 180 and 270°) keeping the sample-to-detector distance fixed at 6.145 cm and the detector position (2θ) fixed at –28°. The X-ray data acquisition was monitored by SMART program.<sup>16</sup> All the data were corrected for Lorentz-polarization effects using SAINT programs.<sup>16</sup> A semi-empirical absorption correction (multi-scan) based on symmetry equivalent reflections was applied using the SADABS.<sup>16</sup> Lattice parameters were determined from least-squares analysis of all reflections. The structures were solved by direct methods and refined by full matrix least squares, based on *F*<sup>2</sup>, using SHELX-97 software package.<sup>17</sup> All H atoms were placed in geometrically idealized positions (with C–H = 0.98 Å for inositol ring H atoms and orthoformate H atoms H7 and H21; C–H = 0.93 Å for aromatic H atoms; C–H = 0.97 Å for methylene H atoms) and constrained to ride on their parent atoms with *U*<sub>iso</sub>(H) = 1.2*U*<sub>eq</sub>(C). The O–bound H atoms were located in difference Fourier maps and refined isotropically. The refined O–H distances were in the range 0.77(3)–0.91(6) Å. In the form I crystals, the hydroxyl bond length O6–H6' was restrained to 0.86(3) Å using the DFIX command. Molecular and packing diagrams were generated using ORTEP-32<sup>18</sup> and Mercury CSD 2.3,<sup>19</sup> respectively. Geometrical calculations were performed using SHELXTL and PLATON.<sup>20</sup> The crystallographic data are summarized in Table 1.

### Results and discussion

Monobenzyl ethers **4–6** of *myo*-inositol orthoesters **1–3** were prepared (Scheme 1) and the stored samples were analyzed for purity/presence of impurities. The benzyl ether **4** was always obtained as a gum and the samples were usually stored at low temperature (0 to –20 °C) or as solution in dichloromethane. We obtained a solid (sample **4C**) on storage of the gummy benzyl ether **4** for long periods of time. The sample **4C** had different solubility characteristics in common organic solvents compared to the gum (sample **4A**) from which these solids formed. For



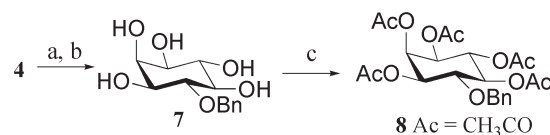
**Scheme 1** Synthesis of racemic 4-*O*-benzyl-*myo*-inositol-1,3,5-orthoesters. (a) DMF, NaH, benzyl bromide (BnBr), 2 h, 80–90%.

**Table 1** Crystallographic data for dimorphs of **4**

	Form I	Form II
Chemical formula	C <sub>14</sub> H <sub>16</sub> O <sub>6</sub>	C <sub>14</sub> H <sub>16</sub> O <sub>6</sub>
<i>M<sub>r</sub></i>	280.27	280.27
<i>T</i> /K	297(2)	297(2)
Morphology	Plate	Plate
Crystal size	0.22 × 0.12 × 0.07	0.17 × 0.15 × 0.08
Crystal system	Orthorhombic	Monoclinic
Space group	<i>Pbca</i>	<i>P2<sub>1</sub>/c</i>
<i>a</i> /Å	10.460(5)	10.4043(17)
<i>b</i> /Å	11.536(5)	13.720(2)
<i>c</i> /Å	42.364(19)	10.3515(17)
$\alpha$ (°)	90	90
$\beta$ (°)	90	118.031(3)
$\gamma$ (°)	90	90
<i>V</i> /Å <sup>3</sup>	5112(4)	1304.3(4)
<i>Z</i>	16	4
<i>D<sub>s</sub></i> /g cm <sup>-3</sup>	1.457	1.427
$\mu$ /(mm <sup>-1</sup> )	0.115	0.112
<i>F</i> (000)	2368	592
<i>T<sub>min</sub></i>	0.975	0.981
<i>T<sub>max</sub></i>	0.992	0.991
<i>h, k, l</i> (min, max)	(-11, 12), (-13, 13), (-46, 50)	(-12, 12), (-16, 16), (-9, 12)
Reflns collected	24154	6531
Unique reflns	4500	2307
Observed reflns	2952	1591
<i>R<sub>int</sub></i>	0.0616	0.0583
No. of parameters	377	189
GoF	1.024	1.224
<i>R<sub>1</sub></i> [ <i>I</i> > 2σ( <i>I</i> )]	0.0513	0.0852
<i>wR<sub>2</sub></i> [ <i>I</i> > 2σ( <i>I</i> )]	0.1163	0.1454
<i>R<sub>1</sub></i> _all data	0.0867	0.1280
<i>wR<sub>2</sub></i> _all data	0.1343	0.1581
$\Delta\rho_{\max}$ , $\Delta\rho_{\min}$ /e Å <sup>-3</sup>	0.45, -0.26	0.20, -0.21
CCDC No.	848918	848919

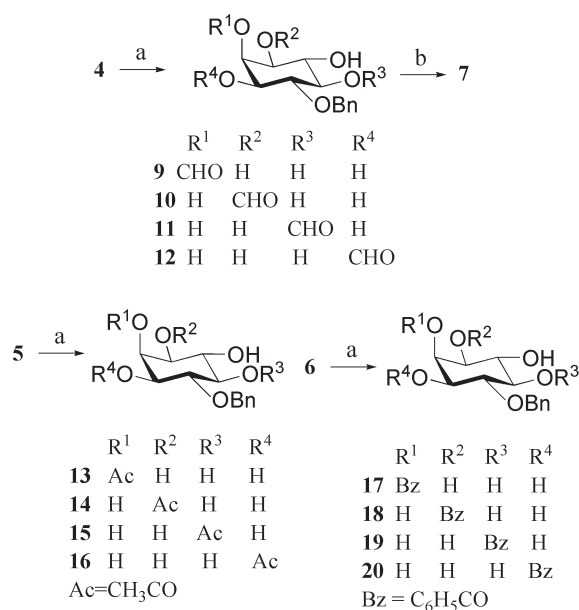
example, sample **4A** was completely soluble in dichloromethane and methanol, while the sample **4C** was sparingly soluble in dichloromethane. The sample **4C** was, however, completely soluble in methanol. Some of the samples of **4** which had been stored for longer periods of time revealed the presence of well defined crystals (form I and form II). Interestingly, the solubility characteristics of these crystals were similar to those of the gums (sample **4A**) from which crystals had formed. Hence, we systematically analyzed the samples of 4-*O*-benzyl ethers **4–6** of *myo*-inositol-1,3,5-orthoesters.

The FT-IR spectra of the gummy (sample **4B**, up to 4 weeks) and the amorphous (sample **4C**, up to 2 years) samples of **4** revealed peaks between 1710 and 1730 cm<sup>-1</sup>, suggesting the presence of a carbonyl group, though the benzyl ether **4** is devoid of carbonyl groups. The FT-IR spectrum of freshly prepared samples of **4** (sample **4A**), however, did not indicate the presence of carbonyl group. Heating (120–130 °C) sample **4A** also led to the formation of a mixture of products similar to the samples of **4** stored for long periods of time (samples **4B** or **4C**), as revealed by a comparison of the IR spectra. A comparison of the <sup>1</sup>H NMR spectra of the same samples (**4A**, **4B**, **4D**) indicated the appearance of signals between δ5 and δ6, (which indicated the formation of esters, see below) of inositol. Broadening of signals was also observed due to the formation of a mixture of inositol derivatives. The <sup>1</sup>H NMR spectra and the PXRD patterns of the solid samples **4D** and **4E** were very similar to that of Form I crystals, indicating that they were in fact microcrystalline forms of the latter crystals.

**Scheme 2** (a) Store for several months or heat at 130 °C for 12 h; (b) chromatography; (c) pyridine, acetic anhydride, ambient temperature, 48 h.

Chromatographic purification of the sample **4C** yielded small quantities of a polar component along with the pure benzyl ether **4**. However, the FT-IR spectra of both these compounds did not reveal the presence of a carbonyl group. Acetylation of the polar component yielded a penta-acetate, whose structure was established to be **8** (Scheme 2) based on its spectral data. Hence, the precursor of **8** isolated after chromatography from the sample **4C** must be racemic 4-*O*-benzyl-*myo*-inositol (**7**). This explains the insolubility of the solid sample **4C** in non-polar solvents such as dichloromethane and its solubility in polar solvents like methanol, as mentioned earlier.

The results described above, however, did not account for the presence of carbonyl group (as indicated in their IR spectra) in stored samples of **4**. Hence we also examined the samples of the benzyl ethers **5** and **6** of *myo*-inositol-1,3,5-orthoacetate and orthobenzoate.<sup>21</sup> The benzyl ethers **5** and **6**, which were obtained as gums, were heated and IR and NMR spectra of the resulting samples were analyzed. A comparison of the IR spectra of the orthoesters **5** and **6**, before and after heating showed an increase in intensity of the peak due to the ester carbonyl group. The <sup>1</sup>H NMR spectra of the same samples also indicated the appearance of signals between δ5 and δ6, which indicated the formation of esters (acetates and benzoates, Scheme 3) of inositol. Broadening of signals was also observed due to the formation of a mixture of inositol derivatives. Analysis of older samples of the benzyl ethers **5** and **6** by IR spectroscopy also showed the presence of carbonyl group in them, as observed in aged samples of **4**. From

**Scheme 3** Formation of esters from **4**, **5** and **6**. (a) Store for several months or heat for 12 h; (b) chromatography.

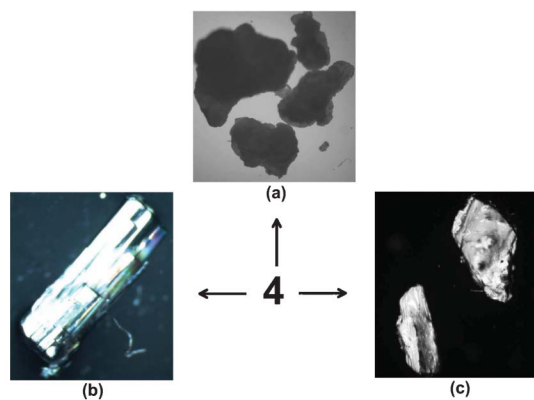


**Fig. 1** Photomicrographs of solid samples of **4**. (a) amorphous solid (sample **4C**); (b) Form I crystals; (c) Form II crystals.

a comparison of the results obtained by the analysis of the samples of the benzyl ethers **4–6**, we could infer that the orthoformate **4** gets converted to the corresponding formate esters (**9–12**, Scheme 3) which are stable in the gum (perhaps due to absence of water) but hydrolyze during work-up or chromatography to the corresponding pentol **7**. Esters of formic

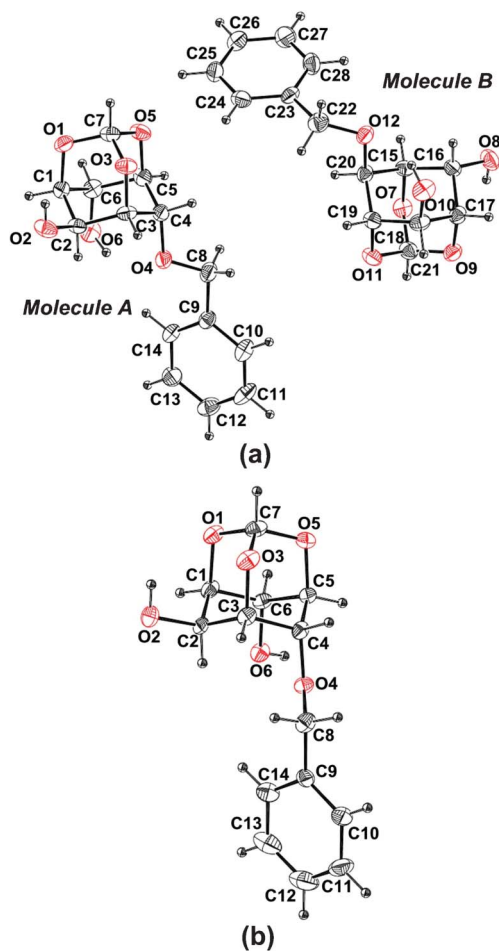


**Fig. 2** Representative ORTEP of molecules in (a) form I and (b) form II crystals. Thermal ellipsoids are drawn at 30% probability and hydrogen atoms are depicted as small spheres of arbitrary radii.

acid are known<sup>22</sup> to be far more labile to hydrolysis as compared to other carboxylic acid esters. It is pertinent to mention here that the instability of *myo*-inositol orthoesters has recently been exploited for the regioselective acylation of the C2-hydroxyl group.<sup>23</sup>

Two of the samples (**4A**) stored for extended periods of time revealed the formation of plate-like (form I) and block-shaped crystals (form II, Fig. 1) embedded in the gum. However, slow rate of crystallization (a period of 3 to 4 weeks for form I and 3 to 4 months for form II) initially, prevented us from developing a procedure for obtaining crystals of **4** consistently. Fortunately, we were able to obtain form I crystals of **4** consistently by first cooling the gummy sample to  $-20\text{ }^{\circ}\text{C}$  to obtain a solid

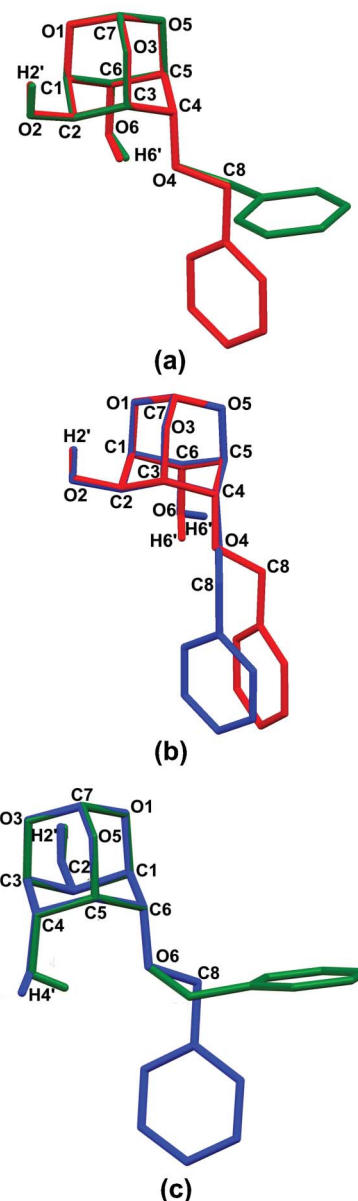


**Fig. 3** The overlap of molecules in (a) the asymmetric unit of form I crystals (red and green), (b) form I (molecule A, red) and form II crystals (blue), (c) form I (molecule B, green) and form II crystals (blue), which show the conformational differences in the functional groups. C-H H-atoms are omitted for the sake of clarity.

(microcrystalline - sample **4E**) and its subsequent crystallization from dichloromethane–light petroleum mixture. Our attempts to crystallize the freshly prepared gummy samples of **4** (without cooling to  $-20\text{ }^{\circ}\text{C}$ ) in the same solvent system failed. Also, we could not obtain form II crystals of **4** reproducibly.

The crystals of form I belong to the orthorhombic space group *Pbca* with an enantiomorph pair of independent molecules in the asymmetric unit (Fig. 2a), while form II crystals are monoclinic, space group *P2<sub>1</sub>/c* (Fig. 2b). The two symmetry-independent molecules in the crystal structure of form I show significant difference in the torsion angle associated with the 4-*O*-benzyl group, C4–O4–C8–C9 ( $\sim 97^{\circ}$ ) while the torsional differences associated with the hydroxyl groups C1–C2–O2–H2' ( $\sim 6^{\circ}$ ) and C1–C6–O6–H6' ( $\sim 12^{\circ}$ ) are small (Fig. 3a). The molecular overlap of form I (molecule A) and form II reveals conformational changes in the C6-hydroxyl group and the benzyl group (Fig. 3b); the difference in torsional angles C1–C6–O6–H6' and C4–O4–C8–C9 being  $\sim 86^{\circ}$  and  $9^{\circ}$  respectively. The torsional angle differences for the C6-hydroxyl and C4-benzyl groups in the molecular overlay of the form I (molecule B) and form II crystals (Fig. 3c) are  $\sim 74^{\circ}$  and  $106^{\circ}$ , respectively. These conformational changes drive the molecular association in the dimorphs. The calculated powder X-ray diffraction patterns of the dimorphs also reveal the structural differences between the two forms (see ESI†).

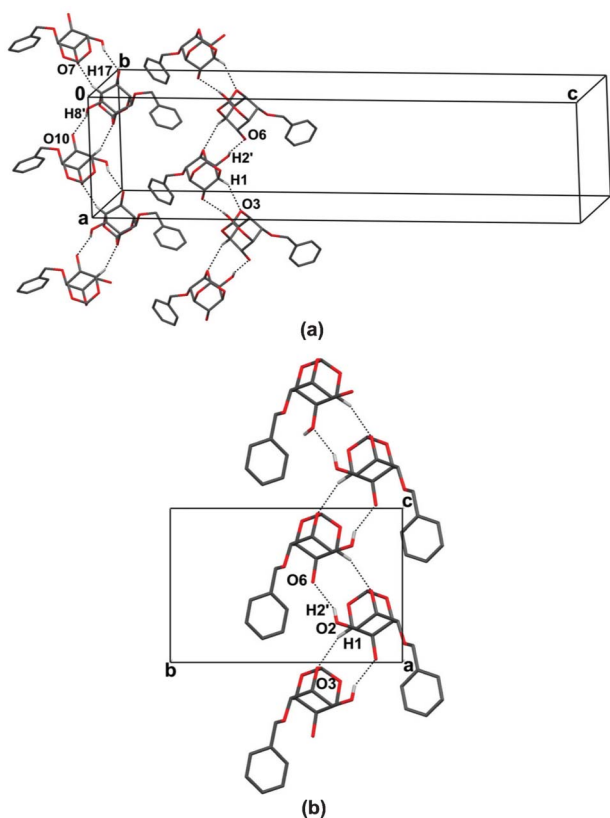


**Fig. 4** Intermolecular O–H $\cdots$ O hydrogen bonding in crystals of **4**; (a) form I, consisting of separate chains of glide and screw related molecules along the *a*-axis, and (b) form II, glide related molecules associated along the *c*-axis. Dotted lines represent O–H $\cdots$ O and C–H $\cdots$ O interactions. H-atoms not involved in hydrogen bonding are omitted for the sake of clarity.

Vasella and co-workers<sup>24,25</sup> investigated the intramolecular hydrogen bonding in **4** by an analysis of their FT-IR spectra in CCl<sub>4</sub> and DMSO solutions. A strong intramolecular hydrogen bond was observed between the C6-hydroxyl group and the oxygen atom O4 (O6–H6' $\cdots$ O4) while the C2–OH group exhibited weaker hydrogen bonding with the orthoester oxygen atoms O1 and O3 in solution. In the crystalline state the hydrogen bonding between the C6-hydroxyl group and the C4-oxygen atom is intramolecular in form I (paralleling that in solution) and intermolecular in form II crystals. The identical orientation of the C2-hydroxyl group in the dimorphs results in similar hydrogen bonding interactions, with the axial hydroxyl group of a glide-related molecule (O2–H2' $\cdots$ O6, in case of molecule A in form I and molecules in form II crystals) or a screw related molecule (O8–H8' $\cdots$ O10, in case of molecule B in form I) forming an O–H $\cdots$ O linked molecular chain (Fig. 4). Identical supporting C–H $\cdots$ O interactions between inositol ring proton and the orthoformate oxygen atom (C1–H1 $\cdots$ O3 and C17–H17 $\cdots$ O7, Fig. 4) along the molecular chains are also observed in both the forms. In form I crystals, adjacent chains of glide related molecules (molecule A) are linked by a pair of short and linear C–H $\cdots$ O interactions (C7–H7 $\cdots$ O2 and C2–H2 $\cdots$ O5) while chains of screw related molecules (molecule B) are linked

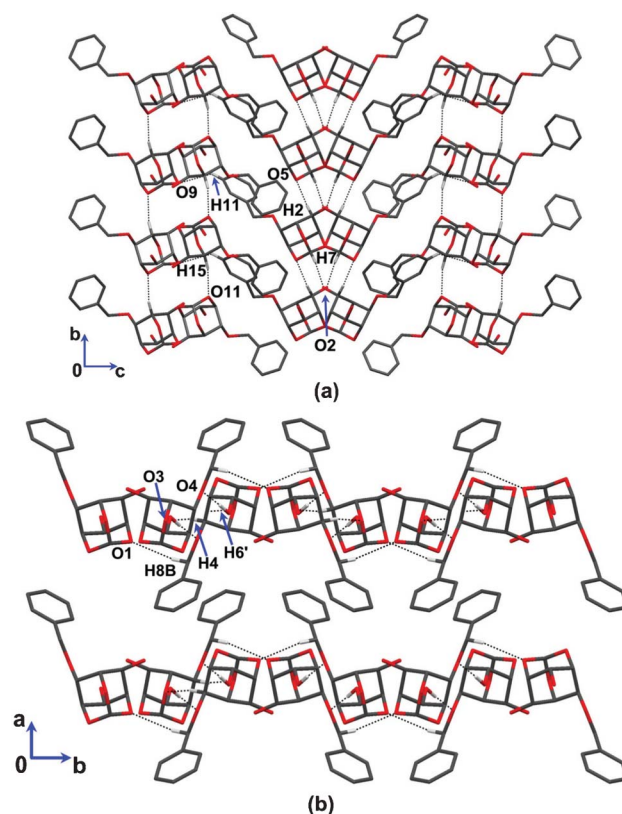


**Fig. 5** Molecular packing in crystals of **4**; (a) form I: chains of glide and screw related molecules along the *b*-axis are linked by C–H $\cdots$ O interactions. Adjacent chains along the *c*-axis are linked by C11–H11 $\cdots$ O9 contacts, and (b) form II: chains of glide related molecules are linked by O–H $\cdots$ O and C–H $\cdots$ O interactions. Dotted lines represent hydrogen bonding interactions. H-atoms not involved in hydrogen bonding are omitted for the sake of clarity. The blue arrows indicate the atoms referred to by the atom labels.

**Table 2** Geometrical parameters for H-bonding interactions<sup>b</sup>

Form	D–H⋯A	D–H (Å)	H⋯A (Å)	D⋯A (Å)	D–H⋯A (°)	
I	O2–H2'⋯O6 <sup>i</sup>	0.77(3)	2.21(3)	2.910(3)	152(3)	
	O6–H6'⋯O4 <sup>ii</sup>	0.86(3)	2.10(3)	2.802(3)	139(3)	
	O8–H8'⋯O10 <sup>iii</sup>	0.81(4)	2.25(3)	3.004(3)	155(4)	
	O10–H10'⋯O12 <sup>iv</sup>	0.88(4)	2.05(4)	2.804(3)	143(4)	
	C1–H1⋯O3 <sup>v</sup>	0.98	2.58	3.380(3)	139	
	C2–H2⋯O5 <sup>vi</sup>	0.98	2.48	3.459(3)	174	
	C7–H7⋯O2 <sup>vii</sup>	0.98	2.22	3.193(4)	170	
	C11–H11⋯O9 <sup>viii</sup>	0.93	2.57	3.296(4)	136	
	C15–H15⋯O11 <sup>ix</sup>	0.98	2.42	3.366(3)	164	
	O2–H2'⋯O6 <sup>x</sup>	0.84(6)	2.08(5)	2.839(4)	151(6)	
	O6–H6'⋯O4 <sup>xi</sup>	0.91(7)	1.92(7)	2.824(4)	175(6)	
	II	C1–H1⋯O3 <sup>x</sup>	0.98	2.44	3.364(5)	158
		C4–H4⋯O3 <sup>xi</sup>	0.98	2.55	3.495(4)	161

<sup>a</sup> Intramolecular interaction. <sup>b</sup> Symmetry codes: (i)  $x - 1/2, y, -z + 1/2$ ; (ii)  $x + 1/2, -y + 1/2, -z$ ; (iii)  $x + 1/2, y, -z + 1/2$ ; (iv)  $-x + 3/2, y + 1/2, z$ ; (v)  $-x + 1, y - 1/2, -z + 1/2$ ; (vi)  $-x, -y + 1, -z$ ; (vii)  $-x + 1/2, y - 1/2, z$ ; (viii)  $x, -y + 1/2, z + 1/2$ ; (ix)  $-x + 1, -y, -z$ ; (x)  $x, -y + 1/2, z - 1/2$ ; (xi)  $-x + 1, -y, -z + 1$ .

by moderately strong C15–H15⋯O11 contacts along the *b*-axis (Fig. 5a). Adjacent molecular chains are connected by weak C11–H11⋯O9 interactions along the *c*-axis. In form II crystals the O–H⋯O bonded molecular chains are linked along the *b*-axis by short and linear O6–H6'⋯O4 and C4–H4⋯O3 contacts (Table 2) and weak C8–H8B⋯O1 interactions (Fig. 5b).

Thus, strong intramolecular O–H⋯O interactions observed in solutions of **4** are carried over to the crystals of form I, which also exhibit a faster rate of crystallization than the form II crystals. The dimorphs exhibit similar patterns of O–H⋯O hydrogen bonding involving the C2-hydroxyl groups in forming molecular chains, however, the conformational differences in the C6-hydroxyl and C4-benzyl groups in the dimorphs result in dissimilar modes of packing in their crystals. Studies of the crystal structure of polymorphic systems, with multiple molecules in the asymmetric unit along with the patterns of molecular aggregation in solution and solid-state could help in understanding the enigmatic processes of nucleation and crystal growth.

## Conclusions

Analysis of the samples of racemic 4-*O*-benzyl-*myo*-inositol-1,3,5-orthoformate (**4**) stored for longer periods of time revealed the reason for its slow rate of crystallization and helped us to develop a procedure to obtain well defined crystals of a compound, until now reported as a gum. The results suggest that the products formed on cleavage of the orthoformate during storage prevent the crystallization of **4** and hence, it exists as a gum or turns to an amorphous solid on storage. Comparison of the structures of the dimorphs obtained show that conformational flexibility in even a small functional group such as the hydroxyl group can result in dissimilar molecular arrangement in the crystal lattice, leading to conformational dimorphs.<sup>26,27</sup> The enhanced molecular stability for **4**, imparted by the crystal lattice as compared to the gummy state implies distinction in the molecular aggregation and intermolecular interactions in different states, resulting in an improved stability of molecules in the crystalline state.<sup>14,28,29</sup> There are several instances of small organic molecules exhibiting enhanced reactivity in their crystalline state, relative to solution or

molten states, owing to proper orientation of the reactive functional groups in crystals.<sup>30</sup> Such systems are valuable in organic synthesis and in understanding the reaction mechanisms. The example described in this article demonstrates the opposite, in that the molecules are imparted higher stability (or lower reactivity) in their crystal as compared to the gummy state. This aspect is of relevance in the context of understanding the stability of small molecules such as drugs and drug intermediates, which require storage over longer periods of time, without compromising on their purity and pharmaceutical performance. The latter could deteriorate due to changes in content or composition resulting from lack of molecular stability.

## Acknowledgements

We thank the Department of Science and Technology, New Delhi, India, for financial support. RS and SK are recipients of senior research fellowship from the University Grants Commission, and the Council of Scientific and Industrial Research, New Delhi, India, respectively.

## References

- B. V. L. Potter and D. Lampe, *Angew. Chem. Int. Ed. Engl.*, 1995, **34**, 1933–1972.
- K. M. Sureshan, M. S. Shashidhar, T. Praveen and T. Das, *Chem. Rev.*, 2003, **103**, 4477–4503.
- S. Kim, S. Lee and C. Cheong, *Bull. Korean Chem. Soc.*, 2004, **25**, 1578–1580.
- B. Kilbas and M. Balci, *Tetrahedron*, 2011, **67**, 2355–2389.
- Phosphoinositides: chemistry, biochemistry and biomedical applications*, Bruzik, K. S. Ed. ACS symposium series, 718, American Chemical Society, Washington DC, USA, 1999.
- C. M. Longo, Y. Wei, M. F. Roberts and S. J. Miller, *Angew. Chem. Int. Ed.*, 2009, **48**, 4158–4161.
- P. A. Jordan, K. J. Kayser-Bricker and S. J. Miller, *PNAS*, 2010, **107**, 20620–20624.
- A. E. Koumbis, C. D. Duarte, C. Nicolau and J. M. Lehn, *Chem. Med. Chem.*, 2011, **6**, 169–180.
- S. Devaraj, R. C. Jagdhane and M. S. Shashidhar, *Carbohydr. Res.*, 2009, **344**, 1159–1166 and references cited therein.
- D. C. Billington, R. Baker, J. J. Kulagowski, I. M. Mawer, J. P. Vacca, S. J. deSolms and J. R. Huff, *J. Chem. Soc., Perkin Trans. 1*, 1989, 1423–1429.
- C. Murali, M. S. Shashidhar, R. G. Gonnade and M. M. Bhadbhade, *Chem.—Eur. J.*, 2009, **15**, 261–269.
- G. Baudin, B. I. Glänzer, K. S. Swaminathan and A. Vasella, *Helv. Chim. Acta*, 1988, **71**, 1367–1378.
- L. T. Padiyar, Y. Wen and S. Hung, *Chem. Commun.*, 2010, **46**, 5524–5526.
- B. P. Gurale, S. Krishnaswamy, V. Kumar and M. S. Shashidhar, *Tetrahedron*, 2011, **67**, 7280–7288.
- (a) M. A. L. Podeschwa, O. Plettenberg and H. Altenbach, *Eur. J. Org. Chem.*, 2005, 3116–3127; (b) J. Gigg, R. Gigg, S. Payne and R. Conant, *J. Chem. Soc., Perkin Trans. 1*, 1987, 423.
- Bruker 2003. SADABS Version 2.05, SMART Version 5.631 and SAINT Version 6.45. Bruker AXS Inc., Madison, Wisconsin, USA.
- G. M. Sheldrick, *Acta Crystallogr., Sect. A: Found. Crystallogr.*, 2008, **64**, 112–122.
- L. J. Farrugia, *J. Appl. Crystallogr.*, 1997, **30**, 565.
- C. F. Macrae, P. R. Edgington, P. McCabe, E. Pidcock, G. P. Shields, R. Taylor, M. Towler and J. J. van de Streek, *Appl. Crystallogr.*, 2006, **30**, 453–457.
- A. L. Spek, *J. Appl. Crystallogr.*, 2009, **65**, 148–155.
- C. Murali, M. S. Shashidhar and C. S. Gopinath, *Tetrahedron*, 2007, **63**, 4149–4155.

- 22 R. W. Taft Jr., *J. Am. Chem. Soc.*, 1952, **74**, 3120–3128.
- 23 A. M. Vibhute, A. Vidyasagar, S. Sarala and K. M. Sureshan, *Chem. Commun.*, 2012, **48**, 2448–2450.
- 24 P. Uhlmann and A. Vasella, *Helv. Chim. Acta*, 1992, **75**, 1979–1994.
- 25 B. Bernet and A. Vasella, *Helv. Chim. Acta*, 2000, **83**, 995–1021.
- 26 R. M. Ibberson, S. Parsons, D. R. Allen and A. M. T. Bell, *Acta Crystallogr. Sect B*, 2008, **64**, 573–582.
- 27 S. Krishnaswamy, R. G Gonnade, M. M. Bhadbhade and M. S. Shashidhar, *Acta Crystallogr. Sect. C*, 2009, **65**, o54–o57.
- 28 M. F. Beristain, S. Fomine and T. Ogawa, *Mol. Cryst. Liq. Cryst.*, 2006, **447**, 251–263.
- 29 G. Kaupp, *J. Phys. Org. Chem.*, 2008, **21**, 630–643.
- 30 S. Krishnaswamy, M. S. Shashidhar and M. M. Bhadbhade, *CrystEngComm.*, 2011, **13**, 3258–3264 and references cited therein.